Single Crystals of the Poly(L-lactide) Block and the Poly(ethylene glycol) Block in Poly(L-lactide)−poly(ethylene glycol) Diblock Copolymer

Junliang Yang, Ting Zhao, Yunchun Zhou, Leijing Liu, Gao Li,* Enle Zhou, and Xuesi Chen

State Key Laboratory of Polymer Physics and Chemistry, Changchun Institute of Applied Chemistry, Graduate School of Chinese Academy of Sciences, Chinese Academy of Sciences, Changchun 130022, P. R. China

Received November 27, 2006; Revised Manuscript Received February 5, 2007

ABSTRACT: Single crystals of the poly(L-lactide) (PLLA) block and the poly(ethylene glycol) (PEG) block in poly(L-lactide)−poly(ethylene glycol) diblock copolymer were obtained by melt crystallization. The morphology, structure, and evolution process of the single crystals were investigated using transmission electron microscopy (TEM), selected-area electron diffraction (SAED), and real-time atomic force microscopy (AFM). Two types of crystal morphology were obtained. One was the regular morphology of a single crystal: lozenge-spiral dislocation, lozenge multilayer, and hexagonal (or truncated-lozenge) multilayer, which was layer-by-layer structure. The foregoing crystallization of the PLLA block determined the regular morphology of single crystal. The other type of crystal morphology was that the layer-dendritic crystal, which was affirmed to be the PEG crystal by real-time AFM, formed at the edge of the regular single crystal and grew along some certain directions on the crystal surface of the PLLA block. The forming of layer-dendritic crystal was through the reorganization of metastable phase crystal of the PEG block. The SAED results indicated that the (001) plane of the PLLA crystal was parallel to the (10−4) plane of the PEG crystal and the substrate. The foregoing crystallization of the PLLA block had an effect on the crystal orientation of the PEG block.

Introduction

Double crystalline block copolymers with good properties, such as biodegradability, biocompatibility, innocuity, tissue absorbability, and so on, have attracted many researchers' attention because of their potential application in medical areas. Therefore, in recent years, many double crystalline block copolymers have been studied extensively,[1−20] such as poly(L-lactide)-*b*-poly(ϵ-caprolactone) (PLLA−PCL),[4−8] poly(L-lactide)-*b*-poly(ethylene glycol) (PLLA−PEG),[9−15] poly(ethylene glycol)-*b*-poly(caprolactone) (PEG−PCL),[16−18] and poly(*p*-dioxanone)-*b*-poly(ϵ-caprolactone) (PPDX−PCL).[19,20] The crystallization behavior of double crystalline block copolymers is complicated because two crystallization processes work cooperatively when the copolymer is quenched from the homogeneous or microphase-separated melt state into various temperatures below the melting temperatures of both blocks. If the melting temperatures of both blocks are very close, for example in the case of PEG−PCL copolymer, the crystallization temperatures of both blocks are also very close, and the crystallization precedence is determined by the relative molecular weight of both blocks. Moreover, simultaneous crystallization of both blocks may occur under some conditions. If the melting temperature of one block is far from that of the other one, especially when the melting temperature of one block is lower than the crystallization temperature of the other, the crystallization of the high-T_m block is from fully amorphous state to amorphous−semicrystalline state, and the crystallization of the low-T_m block is in a three-phase morphology in which two distinct crystalline phases coexist with a mixed amorphous phase. During the crystallization process of the high-T_m block, the low-T_m block acts as a dilute solvent and influences its crystallization. In addition, the accomplished crystallization of the high-T_m block has a restraining effect on the crystallization of the low-T_m block. Moreover, unlike a blend of two crystalline polymers, the two crystallizable blocks of the double crystalline block copolymer are connected by chemical bonds and constrain their activity with each other.

PLLA−PEG block copolymer is one of the most important biomaterials and is widely used in medical areas because of its predominant properties. The melting temperature of the PEG block ($T_m \approx 55$ °C) is much lower than that of the PLLA block ($T_m \approx 165$ °C). Moreover, it is also lower than the crystallization temperature ($T_c \approx 120$ °C) and the glass transition temperature ($T_g \approx 60$ °C) of the PLLA block. Many reports on the properties and application in the medical areas[21−23] and on their condensed state structure[9−15] are available in the literature. However, almost no work about single crystals of the PLLA−PEG block copolymer was reported.[15] In the present study, we investigate the morphology and structure of the single crystals of the PLLA block and the PEG block in the PLLA−PEG diblock copolymer obtained by melt crystallization. Furthermore, the evolution process of the single crystal was also followed by real-time AFM.

Experiment Part

Materials. PLLA−PEG diblock copolymer was prepared by ring-opening polymerization of l-lactide (supplied by Purac) in the presence of monomethoxy-terminated poly(ethylene glycol), which has one methyl end group and a number-average molecular weight of 5000 (supplied by Aldrich), catalyzed by stannous octoate ($Sn(Oct)_2$, 10 mol % relative to PEG) according to the method reported earlier.[24] The molecular weight of the PLLA block was 5000, and the polydispersity (M_w/M_n) of the PLLA−PEG diblock

* To whom correspondence should be addressed. E-mail: ligao@ciac.jl.cn.

10.1021/ma062727z CCC: $37.00
Published on Web 03/14/2007

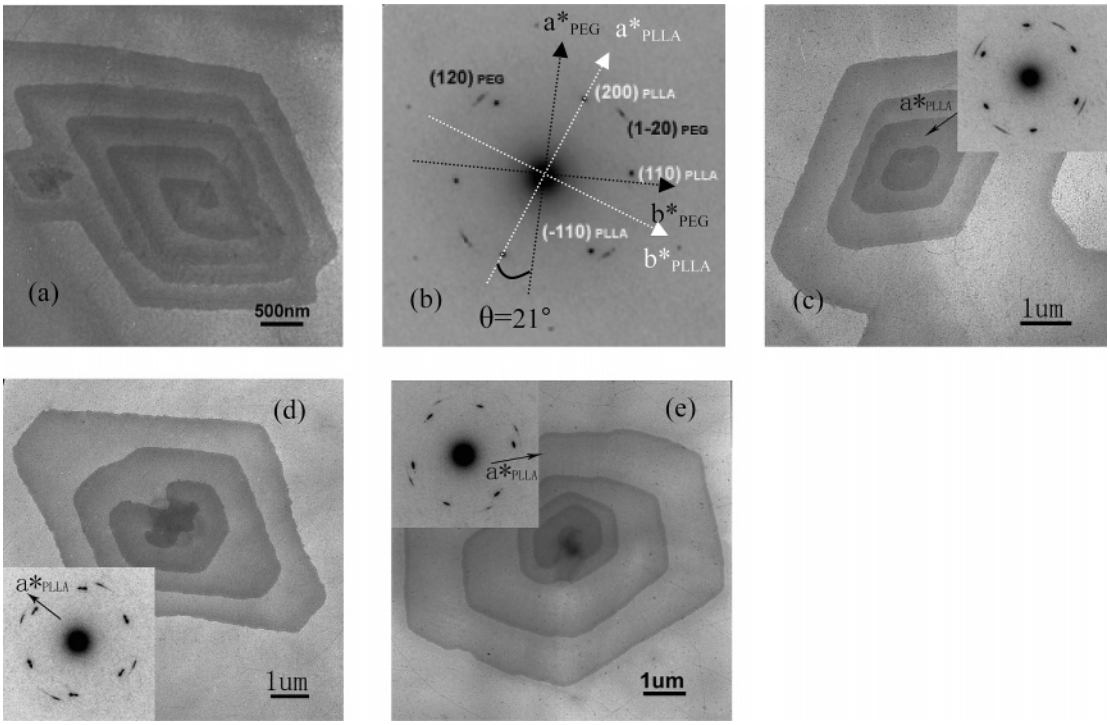

Figure 1. Single-crystal morphologies and corresponding electron diffraction patterns of $LA^5_{50}EG^5_{50}$ diblock copolymer observed by TEM. Specimen was stained by RuO_4. (a) Lozenge-spiral dislocation single crystal; (b) ED pattern of (a) where the angle θ between a^* axes of the PLLA block and the PEG block is 21°; (c) lozenge multilayer single crystal and its ED, $\theta = 22°$; (d) truncated-lozenge multilayer single crystal and its ED, $\theta = 30°$; (e) hexagonal multilayer single crystal and its ED, $\theta = 30°$.

copolymer was 1.25. $LA^5_{50}EG^5_{50}$ represents the PLLA−PEG diblock copolymer, where the superscript indicates the number-average molecular weight of the block in kg/mol and the subscript indicates the content of a particular component in weight percent.

Preparation of $LA^5_{50}EG^5_{50}$ Single Crystal. Using the solution-cast technique, about 0.05 mL of a 0.1% (g/mL) benzene solution of the copolymer was placed on mica and a silicon wafer covered with carbon film, respectively (substrate dimensions, 1 cm × 1 cm). After the benzene was evaporated, the thin film on the substrate was heated to 175 °C and kept for 5 min for complete melt. Then the temperature was decreased to 120 °C rapidly, and the copolymer was allowed to crystallize isothermally for 1 h (the PEG block was in the melt state). Finally, the temperature was decreased to 35 °C rapidly and maintained for 1 h for the PEG block to crystallize. In order to prevent oxidation of the PEG block, melting and annealing of $LA^5_{50}EG^5_{50}$ were both carried out under a nitrogen atmosphere.

TEM Observations. A JEOL JEM-1011 transmission electron microscope (TEM) was used to examine the morphology and electron diffraction of $LA^5_{50}EG^5_{50}$ single crystal at an acceleration voltage of 100 kV. A piece of carbon and polymer film was floated on water and picked up with 400 mesh copper grids. For clearer recognition of morphological features, particularly in multilayer structures, they were stained by RuO_4.

AFM Observations. Real-time experiments of the evolution process of $LA^5_{50}EG^5_{50}$ single crystal on silicon wafer covered with carbon film were performed on a heating stage under vacuum (10^{-5}−10^{-7} Pa) with an SPI 3800/SPA 300HV (Seiko Instrument Inc.) microscope operating in a dynamic force microscope (DFM) mode. AFM height images and phase images were obtained at the same time. A 150 μm scanner and a commercially available SiN_4 cantilever with a spring constant of 42 N/m were used in all real-time experiments. Silver paste was used to fix the specimen on the heating stage. The temperatures of the specimen surface and the heating stage (corresponding to the bottom of the specimen) were monitored. The former was measured by a thermocouple glued on the silicon surface. Temperature gap between the two was found to increase with the temperature. The gap was about 7 °C at above 100 °C. In our study, the surface temperature of the specimen was regarded as the actual recording temperature. The specimen was heated at a rate of about 20 °C/min from room temperature (27 °C) to 175 °C and kept for 10 min at 175 °C, and then it was cooled slowly to find the appropriate temperature for observing the evolution process of $LA^5_{50}EG^5_{50}$ single crystal.

Results and Discussion

Morphology and Structure of Single Crystals. Figure 1 shows the morphologies and corresponding SAED patterns of $LA^5_{50}EG^5_{50}$ single crystals, which were obtained by melt crystallization, in bright field TEM images. After $LA^5_{50}EG^5_{50}$ was melted completely at 175 °C, it was quenched to the crystallization temperature quickly in two steps. The sample was first held at 120 °C for 1 h for the crystallization of the PLLA block and then at 35 °C for 1 h for the crystallization of the PEG block. Single crystals with lozenge-spiral dislocation, lozenge multilayer, and hexagonal (or truncated-lozenge) multilayer were all obtained simultaneously. Parts a and c of Figure 1 are TEM images of lozenge-spiral dislocation and lozenge multilayer single crystals, respectively. Figure 1d shows a lozenge multilayer single crystal with two clearly truncated, which is also called truncated-lozenge multilayer single crystal. Figure 1e is a hexagonal multilayer single crystal whose truncated area becomes bigger. Close examination reveals that there is a step in the crystals where these new sectors and consequently the truncation face starts and develops. Thus, growth conditions must have changed at that stage. The above morphology results are similar to that of Iwata and Doi[25] about the PLLA homopolymer. They reported that the hexagonal, truncated-lozenge, and lozenge-shaped single crystals with spiral growth were prepared simultaneously from solution crystallization.

It is quite unusual that large single crystals of $LA^5_{50}EG^5_{50}$ diblock copolymer can be obtained by melt crystallization. Generally speaking, single crystals are obtained by solution crystallization while melt crystallization produces spherulites

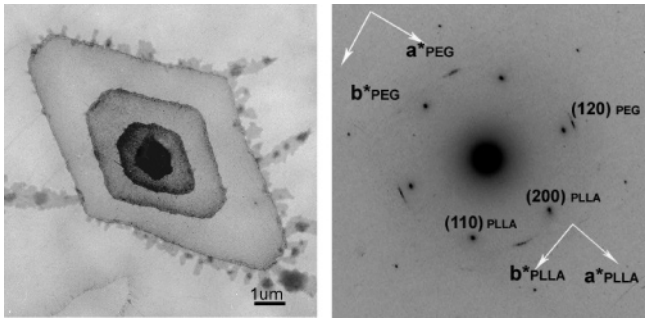

Figure 2. Single-crystal morphology that has layer-dendritic crystals at the edge and its electron diffraction pattern for $LA^5_{50}EG^5_{50}$ diblock copolymer, $\theta = 21°$. Specimen was stained by RuO_4.

for polymers. In solution crystallization, the molecules assume macroconformations close to random coils. Different molecules are separated from each other and arrive on slow crystallization independently, one after another, at the crystal surfaces. These conditions are expected to be suitable for growing large, perfect, and equilibrium single crystals.[26] On the other hand, there are two possible reasons why the PLLA blocks in $LA^5_{50}EG^5_{50}$ diblock copolymer can form single crystals from melt crystallization. Above the PLLA crystallization temperature ($T > 120$ °C), the PEG blocks are melted adequately ($T_m \approx 55$ °C), and the PEG blocks are miscible with the PLLA blocks in the melt state.[15,27] Therefore, the PEG blocks have good mobility and may play a dilute solvent. It is able to provide a favorable environment where the PLLA blocks may assume macroconformations and individual blocks are separated from each other before crystallization. In addition, the molecular weight of the PLLA block is only 5000, which is not high. Thus, the degree of entanglement of the molecular chains is very low in the melt state, which is advantageous for the molecules to fold and form single crystals. After the copolymer crystallizes isothermally at 120 °C, basic regular morphology of $LA^5_{50}EG^5_{50}$ crystal has formed. In other words, the crystallization of the PLLA block determines the morphology of the single crystals because of its foregoing crystallization. At the same time, the PEG blocks are frozen out onto the surface of the PLLA crystals gradually.

After the PLLA blocks have crystallized completely, the temperature is decreased to 35 °C quickly and the PEG blocks crystallize isothermally. Although crystallization of the PEG blocks doubtless occurred on the surface of the PLLA crystals, the basic morphology of single crystal does not change. This regular morphology of single crystal was layer-by-layer structure for both blocks. The foregoing single crystal of the PLLA block may have an induction effect on the forming of the PEG single crystal. But at the same time, the crystallization of the PEG block is restricted in two aspects. First, because of the foregoing crystallization of the PLLA block, crystallization of the PEG block is restricted spatially (geometric restriction). Second, with the chemical bond linking the PLLA and PEG blocks, the molecular diffusion and migration of the PEG blocks are restricted (restriction of chemical bond). Moreover, looking closely to Figure 2, we can observe the layer-dendritic crystals at the edge of the regular single crystal except for the layer-by-layer single crystal. This is another type of crystal morphology compared to the previous one shown in Figure 1. The layer-dendritic crystals will be proved to be PEG crystals in the later part by real-time AFM.

SAED patterns corresponding to single crystals are also shown in Figures 1 and 2. The main feature of the diffraction patterns is that there are two groups of diffractions: the six stronger diffractions belonging to the PLLA crystal and the four strong diffractions with a tetragonal symmetry and a basic spacing corresponding to 4.75 Å belonging to the (120) planes of the PEG crystal. According to our WAXD[28] and SAED results, all of the diffractions of single crystal are well indexed with the α-phase of PLLA (pseudo-orthorhombic, $a = 1.06$ nm, $b = 0.61$ nm, $c = 2.88$ nm)[29] and the monoclinic crystal form of PEG ($a = 0.805$ nm, $b = 1.304$ nm, $c = 1.948$ nm, and $\beta = 125.4°$).[30] The indexed results of the diffraction patterns suggest that the a^*b^* plane of the PLLA crystal is parallel to the a^*b^* plane of the PEG crystal and the substrate. In other words, the (001) plane of the PLLA crystal is parallel to the (10−4) plane of the PEG crystal[31,32] and the substrate. The electronic beam is along c axes (chains direction) of the PLLA and PEG crystals, and the chain stems of the PLLA and PEG blocks in the crystal are perpendicular to the substrate.

Furthermore, it is interesting that the angle θ between the a^* axes of the PLLA and PEG crystals is about 21°−30° in SAED patterns. It indicates that the foregoing crystallization of the PLLA block has an effect on the orientation of the PEG crystal. That is to say, the PLLA crystal determines the growth direction of the PEG crystal. A similar result was also obtained for PCL−PEG block copolymer crystallizing from solution.[33] Is there epitaxial relation between them? Generally speaking, there are two alternative conditions for polymer crystallizes epitaxially on the polymer substrate. Lattice match is one of the basic conditions, and the mismatch (mismatch % = $(d_{depos} - d_{subs})/d_{subs}$) is generally smaller than 15%. Spatial match (incommensurate epitaxy) is another alternative condition. Sometimes spatial match is more important than lattice match. Take the PE/PP system, for example; PE which crystallizes epitaxially on PP is determined by spatial match, and the relation of lattice match is not found.[34,35] Figure 3 is a schematic representation of the epitaxial relation that the PEG block crystallizes on the PLLA crystal. Figure 3c shows the angle between the a^* axes of the PLLA and PEG crystals is about 30°. We should pay attention to Figure 4. For the PLLA crystal, the angle between ⟨1−10⟩ and a or **a*** axis is also 30°. Therefore, a^*_{PEG} is parallel to ⟨1−10⟩. Along this direction, the mismatch = $(2d_{a^*PEG} - d_{\langle 110\rangle PLLA})/d_{\langle 110\rangle PLLA} = (2 \times 0.656\text{ nm} - 1.223\text{ nm})/1.223\text{ nm} = 7.3\%$. The mismatch is smaller than 15%. Therefore, the condition that the angle is about 30° is advantageous for PEG to crystallize epitaxially on the PLLA crystal. But as the angle is about 21°, it is complicated and difficult to find the obvious relation of lattice match (Figure 3d). Spatial match may play an important role during crystallization of the PEG block. The ditch between the folding chains of the PLLA crystal provides favorable space for the PEG chains to fold and crystallize.

As discussed above, the crystallization of the PLLA block determines the basic morphology of crystals. It should be noticed that there is a layer crystal under the regular single crystals, which is formed on the substrate, and we will discuss it later on. From lozenge shape to truncated lozenge shape and finally to hexagonal shape, they should have an intimate relationship. According to the morphologies and the diffraction patterns of the PLLA crystals, the {110} planes are the growth faces of the lozenge-shaped crystals. But the {100} growth faces emerge besides the {110} planes for the truncated-shaped crystals. Therefore, the final morphology is the result of the competition between the growth rates along {100} planes and {110} planes. When these growth rates are almost the same, hexagonal-shaped crystals that are pseudo-hexagonal symmetrical can be obtained, which is shown schematically in Figure 4. The angles between the growth faces are about 60° and 120° for the lozenge-shaped

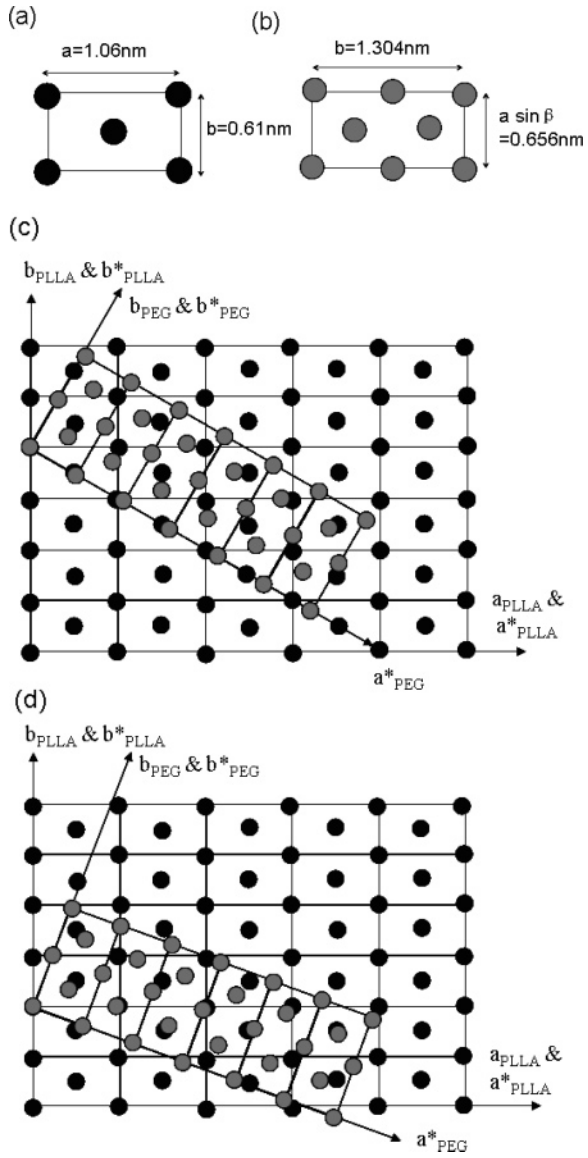

Figure 3. (a) Unit cell of the PLLA crystal along *c* projection; there are two chains per cell. (b) Unit cell of the PEG crystal along *c* projection; there are four chains per cell. (c) The epitaxial relationship of the PEG block crystallizes on the PLLA crystals along *c* projection for the angle $\theta = 30°$. (d) The epitaxial relationship of the PEG block crystallizes on the PLLA crystals along *c* projection for the angle $\theta = 21°$.

single crystal and about 120° for the hexagonal-shaped single crystal. The calculated angles are 60° and 120° between {110} planes and between (110) and (100) planes, respectively (parameters used: $a = 1.06$ nm, $b = 0.61$ nm, $c = 2.88$ nm[29]). The calculated and experimental results are almost equal. It also proves that the foregoing crystallization of the PLLA block determines the basic morphology of the single crystal. The chain folding direction of the crystal growing along {110} is parallel to the {110} growth face, while that of the crystal growing along {100} happens along *a*-axis in the ⟨110⟩ and ⟨1−10⟩ directions successively.

Evolution Process of $LA^5_{50}EG^5_{50}$ Crystal. $LA^5_{50}EG^5_{50}$, which is a type of double crystallizable diblock copolymer, has a complicated crystallization process. During the crystallization process, the $LA^5_{50}EG^5_{50}$ system changes from an amorphous−amorphous state (melt state) to an amorphous−semicrystalline state (after crystallization of the PLLA block) and finally to a semicrystalline−semicrystalline state (after crystallization of the

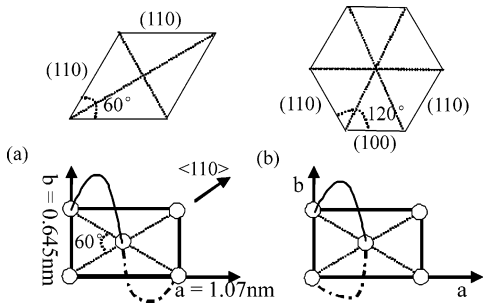

Figure 4. Schematic representation of hexagonal-shaped (or truncated-lozenge shaped) and lozenge-shaped single-crystal lattice of $LA^5_{50}EG^5_{50}$ diblock copolymer: (a) the chain folding direction in the {110} sectors of hexagonal and lozenge single crystals along the ⟨110⟩ direction; (b) the chain folding direction in the {100} sectors of hexagonal single crystals happens along *a*-axis in the ⟨110⟩ and ⟨1−10⟩ directions successively.

PEG block). Both blocks affect their crystallization behavior each other. The foregoing crystallization of the PLLA block severely constrains the crystallization of the PEG block,[28] while the PEG block proffers a dilute solvent for the crystallization of the PLLA block and accelerates its crystallization rate.[36] The evolution process of $LA^5_{50}EG^5_{50}$ crystal was observed using real-time AFM, and the result is shown in Figure 5. In order to observe the crystallization process of the PLLA block in detail, the temperature was decreased from the melt state (175 °C) to 129 °C slowly (at about 0.5 °C /min) and then crystallized isothermally at 129 °C, which is somewhat higher than the crystallization temperature (120 °C) for TEM sample. The PLLA crystal emerges very quickly after annealing at 129 °C for 1592 s (Figure 5a). It is the first time to observe the crystal which formed in 300 s (the time that need to scan an image). The phenomena indicate that it needs a long induction time to nucleate, yet the crystallization rate at the early stage is too high for us to observe the evolution process of the nucleation using real-time AFM. As reported in our other work,[36] the PEG block, introduced acting as a dilute solvent in the crystallization process of the PLLA block, increases the crystallization rate of the PLLA block. At the early stage, two layer crystals have formed: the first layer crystal on the substrate is star-shaped, while the second layer crystal is approximately hexagonal-shaped. The crystal goes on growing with the annealing time increasing at 129 °C, as shown in Figure 5b,c. The growth rate of the first layer is much higher than that of the second layer because of enough material, and the third layer crystal also emerges slowly. The outline of the hexagonal-shaped crystal becomes more distinct, indicating that the crystal is getting more perfect. After annealing at 129 °C for about 1 h, the crystals stop growing.

Then the film is cooled to 35 °C slowly and annealed at this temperature for the crystallization of the PEG block. Some crystals emerge at the edge of the foregoing crystals, and more layer crystals are obtained (Figure 5d). It is doubtless that they result from the crystallization of the PEG block. More and more crystals are obtained at the edge of the second layer crystal and grow along certain directions on the first layer. The morphology of the foregoing regular hexagonal-shaped crystals is changed and takes on the form of layer-dendritic crystals because of the crystallization of the PEG block (Figure 5e,f). Moreover, in Figure 6 we see that the morphology of a regular hexagonal-shaped single crystal remains unchanged, and layer-dendritic crystals form simultaneously at 35 °C. The results are the same with the previous TEM study.

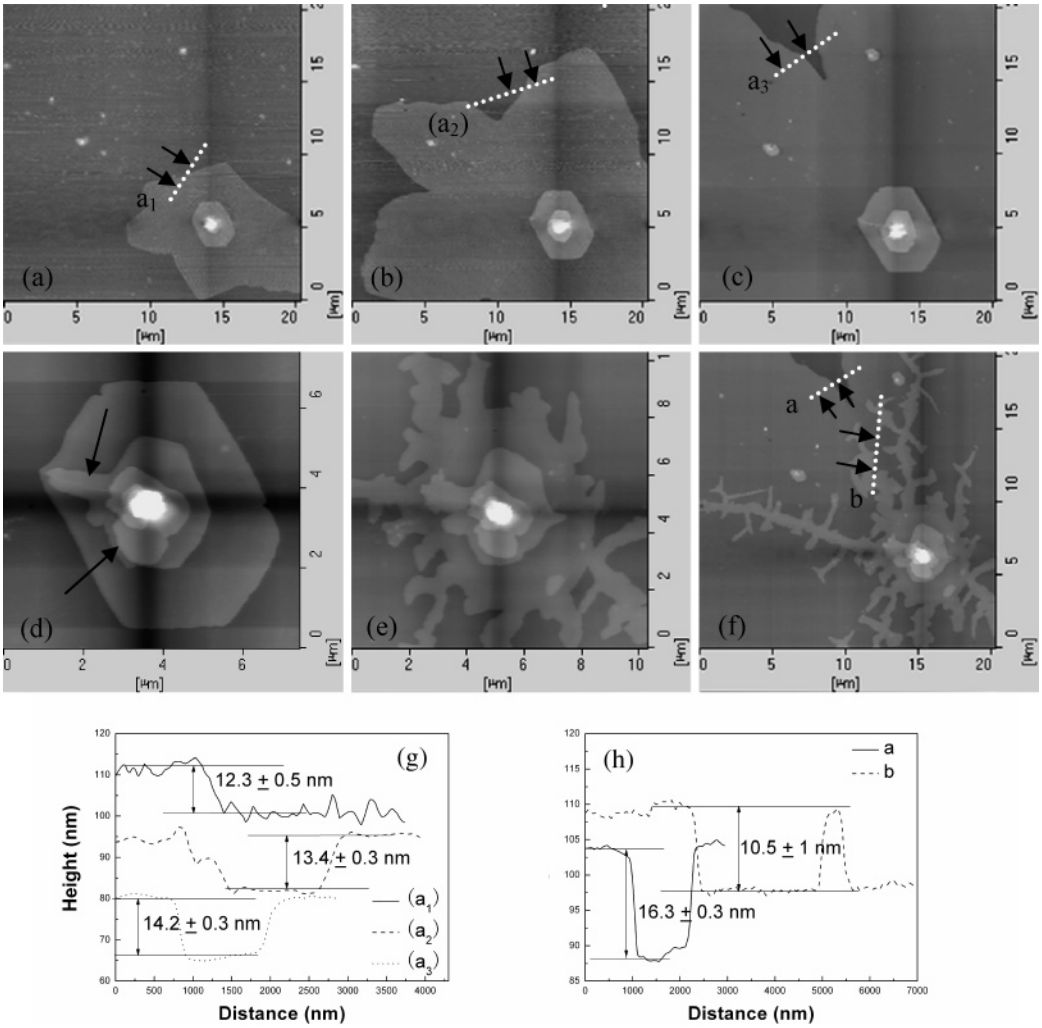

Figure 5. A series of AFM height images and cross-sectional profile data showing the crystallization process of $LA^5_{50}EG^5_{50}$ diblock copolymer. (a), (b), and (c) show the crystallization process of the PLLA block. (d), (e), and (f) show the crystallization process of the PEG block. (a) the first time to find single crystal when $LA^5_{50}EG^5_{50}$ was annealed at 129 °C for 1592 s, the crystal formed in 300 s, but it had a long induction time; (b) annealed at 129 °C for 2610 s; (c) annealed at 129 °C for 3897 s; (d) at 35 °C, the black arrows indicate the PEG crystal that formed just now at the edge of the PLLA crystal; (e) annealed at 35 °C for 1085 s; (f) annealed at 35 °C for 2878 s; (g) cross-sectional profile data corresponding to the dotted lines indicated in (a), (b), and (c); (h) cross-sectional profile data corresponding to the dotted lines indicated in (f).

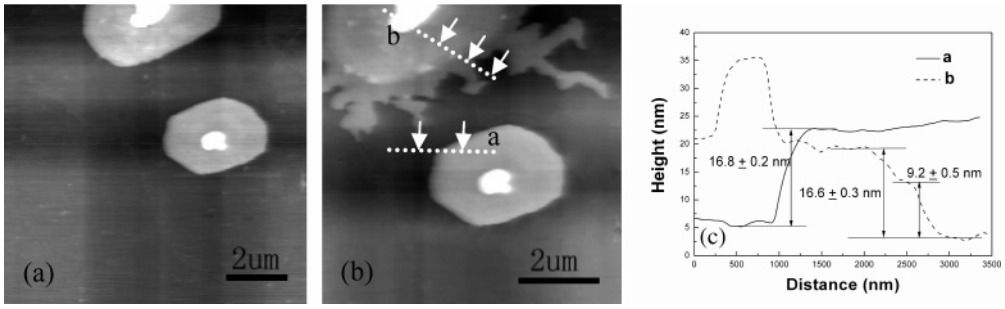

Figure 6. AFM height images and cross-sectional profile data of $LA^5_{50}EG^5_{50}$ single crystal: (a) height image at 120 °C; (b) height image at 35 °C; (c) cross-sectional profile data corresponding to the dotted lines indicated in (b).

It has been reported[37−39] that the crystallization of PEO or PEG can involve noninteger folding (NIF) chain and integer folding (IF) chain. NIF crystals are unstable and will change to the stable IF crystals. The folding number has a close relation with crystallization temperature and crystallization time. The lamellar thickness increases jumpily with the crystallization temperature and crystallization time increasing. Stephen Cheng et al. have proved[39] that PEO crystals grow first as a transient state, and IF chain crystals form later through an isothermal thickening or thinning process depending upon the thermodynamic stability of the NIF crystal. Therefore, the reason for the forming of layer-dendritic crystals for the PEG block is as below: During the crystallization of the PLLA block, the PEG block is frozen out onto the surface of the PLLA crystal, but the material distribution of the PEG block is not uniform. When the temperature is decreased to 35 °C, the amorphous and the metastable phase crystal of the PEG block (NIF crystal) are distributed on the first layer crystal of the PLLA block. At the edge of the regular single crystal, it has more defects and materials. The defects induce the crystallization of the PEG

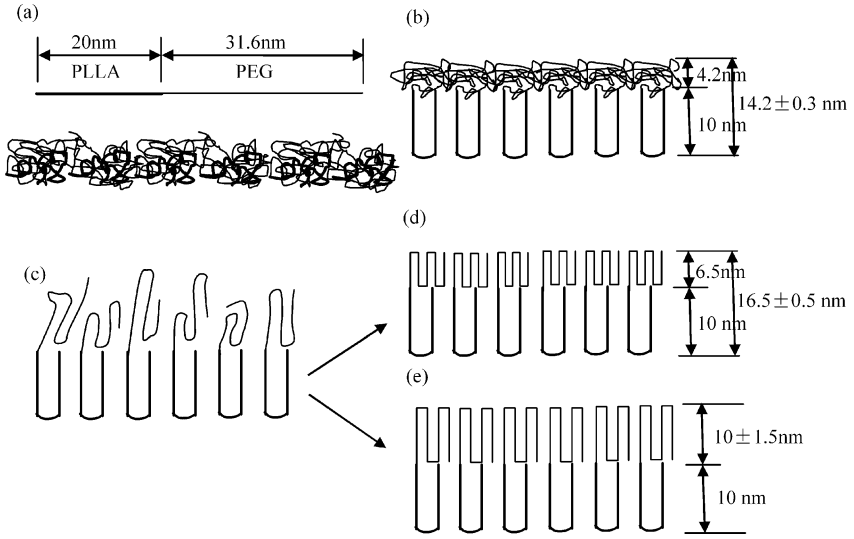

Figure 7. Schematic representation of the structure models for $LA_{50}^{5}EG_{50}^{5}$ at different temperatures: (a) the maximum length of both block molecules in the helical form and the melting state at 175 °C; (b) at temperature between 60 and 129 °C; (c) the metastable phase crystal for the PEG block at 35 °C; (d) the regular morphology crystal at 35 °C; (e) the layer-dendritic crystal at 35 °C.

block and thickening of the metastable phase crystal, and the metastable phase crystal reorganizes along certain directions where there is enough material. Moreover, its reorganization is not free and should be in some domain because it bonds with the PLLA block chemically.

As is known, in crystalline state PLLA chain adopts a 10/3 helical conformation and $c = 2.88$ nm,[29] while PEG is known to take a 7/2 helical conformation and $c = 1.948$ nm.[30] In our case, the molecular weights of both are 5000. If the end-group effect is neglected, the maximum length of the molecules in the fully extended form is $L = L_m N$, where L_m is the length of the repeat unit along the chain axis in the helical state ($L_m = c/n$, n being the repeat number in the length of a unit cell parameter c) and N is the degree of polymerization. Therefore

$$L_{PLLA} = (2.88/10) \times (5000/72) = 20 \text{ nm}$$

$$L_{PEG} = (1.948/7) \times (5000/44) = 31.6 \text{ nm}$$

The PLLA block and the PEG block are homogeneous or weakly segregated (miscible) in the melt state.[15,27] As the temperature is decreased, crystallization is the dominating driving force leading to extensive rearrangement of the morphology when the PLLA block crystallizes first. During its crystallization process, the lamellar thickness increases from 12.3 ± 0.5 nm (Figure 5a) to 13.4 ± 0.3 nm (Figure 5b). After the PLLA block crystallizes completely, the lamellar thickness is 14.2 ± 0.3 nm (Figure 5c), which consists of the lamellar crystal thickness of the PLLA block and the thickness of the amorphous PEG layer if the thickness of the amorphous PLLA block is neglected. The cross-sectional profile data are shown in Figure 5g. When the temperature decreases to 35 °C and the PEG block crystallizes completely, the lamellar thickness increases to 16.5 ± 0.5 nm on average, which now consists of the lamellar crystal thickness of both the PLLA and the PEG blocks if the amorphous layer is neglect. Figures 5h and 6c indicate that the thickness of the layer-dendritic crystal is 10 ± 1.5 nm on average.

Based on these numbers and the SAED results, a schematic representation of the evolution process of two types of crystal morphology is presented in Figure 7. Figure 7a shows the maximum length of the copolymer molecule in the helical form and the coils in the melting state at 175 °C. Figure 7b is $LA_{50}^{5}EG_{50}^{5}$ at a temperature between 60 and 129 °C. Using $l(k)$ represents the length of k folding. At 129 °C, the thickness of the sample is 14.2 ± 0.3 nm, i.e., $l_{PLLA}(k) + l_{\text{melting state of PEG}} = 14.2 \pm 0.3$ nm. Considering the molecular chain length of the PLLA block and the melt state of the PEG block, it is obvious that $k_{PLLA} = 1$, $l_{PLLA}(1) = 10$ nm, and the thickness of the melt PEG block is 4.2 nm. Figure 7c shows the metastable phase crystal for the PEG block at 35 °C. Figure 7d is the regular morphology crystal at 35 °C, and Figure 7e is the layer-dendritic crystal at 35 °C. Considering the molecular chain length of the PEG block and the crystal thickness, for the regular morphology crystal, $l_{PLLA}(1) + l_{PEG}(k) = 16.5 \pm 0.5$ nm and $l_{PEG}(k) = 6.5 \pm 0.5$ nm. Therefore, $31.6/(k_{PEG} + 1) = 6.5 \pm 0.5$ nm and $k_{PEG} = 4$. For the layer-dendritic crystal, $l_{PEG}(k) = 10 \pm 1.5$ nm and $k_{PEG} = 3$.

Conclusion

By using the method of melt crystallization, the single crystals of the PLLA block and the PEG block in $LA_{50}^{5}EG_{50}^{5}$ diblock copolymer were obtained successfully. The single crystals with lozenge-spiral dislocation, lozenge multilayer, and hexagonal (or truncated-lozenge) multilayer are layer-by-layer structure. The foregoing crystallization of the PLLA block determines the crystal morphology. On the other hand, the layer-dendritic crystals also formed at the edge of the regular single crystals and grew along some certain directions. The melt PEG block which acted as a dilute solvent is advantageous to form single crystal of the PLLA block. Furthermore, the PEG block is able to crystallize epitaxially on the PLLA crystal. The (10−4) plane of the PEG crystal is parallel to the (001) plane of the PLLA crystal and the substrate. The angle θ between the a^* axes of the PLLA crystal and the PEG crystal is 21°−30°. The morphology evolution of $LA_{50}^{5}EG_{50}^{5}$ crystal during annealing at 129 and 35 °C was successfully followed using real-time AFM. The layer-dendritic crystals, which formed at 35 °C at the edge of the regular single crystal, result from the reorganization of metastable phase crystal of the PEG block.

Acknowledgment. This work was supported by the fund of the Major Direction Program of the Sciential Inovation Project

of Chinese Academy of Sciences (CAS) (No. KJCX2-SW-H07). We thank Prof. Z. H. Su and Prof. X. N. Yang for offering help during this work.

References and Notes

(1) Hamley, I. W. *Adv. Polym. Sci.* **1999**, *148*, 113.
(2) Loo, Y. L.; Register, R. A. Crystallization within block copolymer mesophases. In *Developments in Block Copolymer Science and Technology*; Hamley, I. W., Ed.; Wiley: New York, 2004.
(3) Müller, A. J.; Balsamo, V.; Arnal, M. L. *Adv. Polym. Sci.* **2005**, *190*, 1.
(4) Hamley, I. W.; Parras, P.; Castelletto. V.; Castillo, R. V.; Müller, A. J.; Pollet, E.; Dubois, P.; Martin, C. M. *Macromol. Chem. Phys.* **2006**, *207*, 941.
(5) Jeong, S. I.; Kim, B. S.; Lee, Y. M.; Ihn, K. J.; Kim, S. H.; Kim, Y. H. *Biomacromolecules* **2004**, *5*, 1303.
(6) Hamley, I. W.; Castelletto, V.; Castillo, R. V.; Müller, A. J.; Martin, C. M.; Pollet, E.; Dubois, Ph. *Macromolecules* **2005**, *38*, 463.
(7) Ho, R. M.; Hsieh, P. Y.; Tseng, W. H.; Lin, C. C.; Huang, B. H.; Lotz, B. *Macromolecules* **2003**, *36*, 9085.
(8) Kim, J. K.; Park, D. J.; Lee, M. S.; Ihn, K. J. *Polymer* **2001**, *42*, 7492.
(9) Fujiwara, T.; Miyamoto, M.; Kimura, Y. *Macromolecules* **2000**, *33*, 2782.
(10) Fujiwara, T.; Kimura, Y. *Macromol. Biosci.* **2002**, *2*, 11.
(11) Fujiwara, T.; Miyamoto, M.; Kimura, Y.; Sakurai, S. *Polymer* **2001**, *42*, 1515.
(12) Lee, S. Y.; Chin, I. J.; Jung, J. S. *Eur. Polym. J.* **1999**, *35*, 2147.
(13) Luo, W.; Li, B. J.; Wang, S. *Polym. Adv. Technol.* **2002**, *13*, 233.
(14) Shin, D.; Shin, K.; Aamer, K. A.; Tew, G. N.; Russell, T. P. *Macromolecules* **2005**, *38*, 104.
(15) Sun, J.; Hong, Z.; Yang, L.; Tang, Z.; Chen, X.; Jing, X. *Polymer* **2004**, *45*, 5969.
(16) He, C.; Sun, J.; Zhao, T.; Hong, Z.; Zhuang, X.; Chen, X.; Jing, X. *Biomacromolecules* **2006**, *7*, 252.
(17) He, C.; Sun, J.; Deng, C.; Zhao, T.; Deng, M.; Chen, X.; Jing, X. *Biomacromolecules* **2004**, *5*, 2042.
(18) Bogdanov, B.; Vidts, A.; Schacht, E.; Berghmans, H. *Macromolecules* **1999**, *32*, 726.
(19) Müller, A. J.; Albuerne, J.; Marquez, L.; Raquez, J. M.; Degee, P.; Dubois, P.; Hobbs, J.; Hamley, I. W. *Faraday Discuss.* **2005**, *128*, 231.
(20) Albuerne, J.; Marquez, L.; Müller, A. J.; Marquez, L. M.; Degee, Ph.; Dubois, Ph.; Castelletto, V.; Hamley, I. W. *Macromolecules* **2003**, *36*, 1633.
(21) Cohn, D.; Younes, H. *J. Biomed. Mater. Res.* **1988**, *22*, 993.
(22) Gref, R.; Minamitake, Y.; Peracchia, M. T.; Trubetskoy, V.; Torchilin, V.; Langer, R. *Science* **1994**, *263*, 1600.
(23) Hagan, S. A.; Coombes, A. G. A.; Garnett, M. C.; Dunn, S. E.; Davies, M. C.; Illum, L.; Davis, S. S. *Langmuir* **1996**, *12*, 2153.
(24) Lee, C. W.; Kimura, Y. *Bull. Chem. Soc. Jpn.* **1996**, *69*, 1787.
(25) Iwata, T.; Doi, Y. *Macromolecules* **1998**, *31*, 2461.
(26) Wunderlich, B. *Macromolecular Physics*; Academic Press: New York, 1976; Vol. 2.
(27) Lai, C. W.; Liu, B. W.; Lin, T. T. *Polymer* **2004**, *45*, 3073.
(28) Yang, J.; Zhao, T.; Cui, J.; Liu, L.; Zhou, Y.; Li, G.; Zhou, E.; Chen, X. *J. Polym. Sci., Part B* **2006**, *44*, 3215.
(29) Hoogsteen, W.; Postema, A. R.; Pennings, A. J.; ten Brinke, G.; Zugenmaier, P. *Macromolecules* **1990**, *23*, 634.
(30) Takahashi, Y.; Tadokoro, H. *Macromolecules* **1973**, *6*, 672.
(31) Baltá Calleja, F. J.; Hay, I. L.; Keller, A. *Polymer* **1966**, *209*, 128.
(32) Lotz, B.; Kovacs, A. J.; Bassett, G. A.; Keller, A. *Polymer* **1966**, *209*, 115.
(33) Sun, J.; Chen, X.; He, C.; Jing, X. *Macromolecules* **2006**, *39*, 3717.
(34) Yan, S.; Petermann, J.; Yang, D. *J. Polym. Sci., Polym. Phys. Ed.* **1997**, *35*, 1415.
(35) Wittmann, J. C.; Lotz, B. *Prog. Polym. Sci.* **1990**, *15*, 909.
(36) Yang, J.; Zhao, T.; Liu, L.; Zhou, Y.; Li, G.; Zhou, E.; Chen, X. *Polym. J.* **2006**, *38*, 1251.
(37) Kovacs, A. J.; Stranpe, C. *Faraday Discuss. Chem. Soc.* **1979**, *68*, 225.
(38) Kovacs, A. J.; Stranpe, C. *J. Cryst. Growth* **1980**, *48*, 210.
(39) Cheng, S. Z. D.; Zhang, A.; Barley, J. S.; Chen, J.; Habenschuss, A.; Zschack, P. R. *Macromolecules* **1991**, *24*, 3937.

MA062727Z